

Denudation rates of the Southern Espinhaço Range, Minas Gerais, Brazil, determined by in situ-produced cosmogenic beryllium-10



Helen N. Barreto ^{a,b,*}, César A.C. Varajão ^a, Régis Braucher ^b, Didier L. Bourlès ^b, André A.R. Salgado ^c, Angélica F.D.C. Varajão ^a

^a Department of Geology, Universidade Federal de Ouro Preto, Campus do Morro do Cruzeiro, CEP: 35.400-000 Ouro Preto/MG, Brazil

^b CEREGE, UMR 6635 CNRS/Université Aix-Marseille, BP 80, 13545 Aix-en-Provence Cedex 4, France

^c Department of Geography, Universidade Federal de Minas Gerais, Av. Antônio Carlos, 6.627 Pampulha, CEP 31270-901 Belo Horizonte/MG, Brazil

ARTICLE INFO

Article history:

Received 7 November 2011

Received in revised form 20 January 2013

Accepted 25 January 2013

Available online 19 February 2013

Keywords:

The Southern Espinhaço Range

Beryllium-10

Cosmogenic nuclide

Denudation rates

Brazil

ABSTRACT

To investigate denudation rates in the southern part of the Espinhaço Range (central-eastern Brazil) and to understand how this important resistant and residual relief has evolved in the past 1.38 My, cosmogenic ¹⁰Be concentrations produced in situ were measured in alluvial sediments from the three main regional basins, whose substratum is composed primarily of quartzites. The long-term denudation rates (up to 1.38 My) estimated from these measurements were compared with those that affect the western (São Francisco River) and eastern (Doce and Jequitinhonha Rivers) basins, which face the West San Francisco craton and the Atlantic, respectively. Denudation rates were measured in 27 samples collected in catchments of different sizes (6–970 km²) and were compared with geomorphic parameters. The mean denudation rates determined in the northern part are low and similar to those determined in the southern part, despite slightly different geomorphic parameter values (catchment relief and mean slope). For the southern catchments, the values are 4.91 ± 1.01 mMy⁻¹ and 3.65 ± 1.26 mMy⁻¹ for the Doce and São Francisco River basins, respectively; for the northern catchments, they are 4.40 ± 1.06 mMy⁻¹ and 3.96 ± 0.91 mMy⁻¹ for the Jequitinhonha and São Francisco River basins, respectively. These low values of denudation rates suggest no direct correlation if plotted against geomorphic parameters such as the catchment area, maximum elevation, catchment relief, average relief and mean slope gradients. These values show that the regional landscape evolves slowly and is strongly controlled by resistant lithology, with similar erosional rates in the three studied basins.

© 2013 Elsevier B.V. All rights reserved.

1. Introduction

Geomorphology studies landscape evolution through the understanding and quantification of the temporal evolution of the underlying processes. Denudation is among the most important of all the processes that affect the morphological evolution of relief (Summerfield, 1998). The term “denudation” refers to all chemical weathering and physical erosion processes that contribute to the lowering of the land surface (Caine, 2004). Until recently, the quantification of denudation over timescales of thousands of years has remained a difficult problem. This difficulty has been overcome with the use of cosmogenic nuclides produced in situ. Accumulating within minerals in the uppermost few meters of the Earth's surface as secondary particles produced by cosmic rays, in situ-produced cosmogenic nuclides can be quantified in terms of not only their exposure duration at or near the surface but also the rates of the processes bringing them to the surface and removing them

from the surface (Brown et al., 1995; Riebe et al., 2000; Granger et al., 2001; Granger and Riebe, 2007). Measurements of cosmogenic nuclide concentrations in rapidly mixed river sediments can be used to determine an average denudation at the scale of the studied river basin (Bierman and Steig, 1996; Granger et al., 1996; Shaller et al., 2001; Von Blanckenburg, 2006; Wittmann and von Blanckenburg, 2009).

In this article, denudation rates given by ¹⁰Be were utilized to evaluate the evolution of an impressive Brazilian water divide, the Espinhaço Range (ER – Von Eschwege, 1832a,b), whose name means “big backbone”. The ER is a 1000-km-long north–south range. It extends across approximately one-fourth of the length of Brazil (Fig. 1). The ER is composed primarily of quartzitic rocks of the Paleo-Mesoproterozoic Espinhaço Supergroup, which exist side-by-side with Neoproterozoic rocks of the São Francisco Supergroup: (i) carbonatic and pelitic rocks of the Bambuí Group and (ii) iron formations and diamictites of the Macaúbas Group (Dussin and Dussin, 1995; Uhlein et al., 1999). The geological substratum is formed by a basement of Archean–Paleoproterozoic gneisses. Geomorphologically, the ER is a resistant quartzitic wall flanked by less resistant rocks. It is a residual landscape that has evolved since the early Proterozoic. The ER has become an important natural water divide for the three largest rivers in SE–NE Brazil,

* Corresponding author at: Department of Geology, Universidade Federal de Ouro Preto, Campus do Morro do Cruzeiro, CEP: 35.400-000 Ouro Preto/MG, Brazil. Tel.: +55 98 32337164.

E-mail address: helennebias@yahoo.com.br (H.N. Barreto).

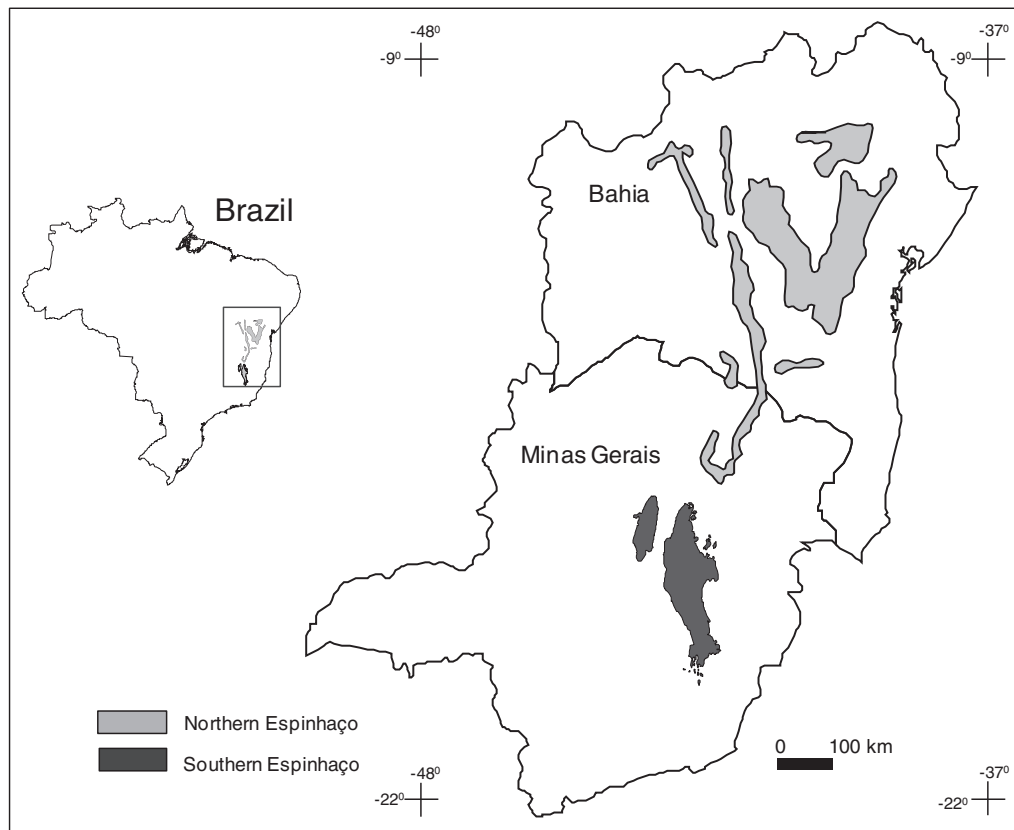


Fig. 1. Location of the Espinhaço Range.

namely, the São Francisco, Jequitinhonha and Doce, with a total area greater than 10^6 km². The Southern Espinhaço Range (SER), located in Minas Gerais state (Fig. 2), was chosen for this study. The concentrations of ¹⁰Be in alluvial sediments were used to quantify the denudation rates on both sides of the SER.

Geomorphologic studies performed in the SER have emphasized the influence of lithology and structure on *landscape-shaping* processes and have attempted to identify planation surfaces (King, 1956; Saadi, 1995; Valadão, 1998). Saadi (1995), based on image interpretation, concluded that the denudation processes are more aggressive in the eastern river basins (Doce and Jequitinhonha) than in the inland river basin (São Francisco). However, these conclusions remain qualitative. The aim of the present article is to study the long-term denudation rates estimated by cosmogenic nuclides to compare the SER erosion rates of the western (São Francisco) and eastern (Doce and Jequitinhonha) basins to understand how this important resistant and residual relief has evolved in the past 1.38 My. The long-term quantification of cosmogenic isotopes, used to study denudation rates by analyzing fluvial sediments, is an important method for understanding landscape evolution (Brown et al., 1995; Matmon et al., 2003; Reuter et al., 2003; Von Blanckenburg, 2006).

2. The Southern Espinhaço Range

Located in Minas Gerais State in the central-east region of Brazil, the SER is approximately 300 km long and extends between 17° 40' S to 19° 40' S and 44° W to 43° 15' W (Fig. 2) (Almeida Abreu, 1995). This range gives rise to three important river basins that represent the major drainage network of Minas Gerais State: the Jequitinhonha, Doce and São Francisco. The Jequitinhonha and Doce River basins lie in the eastern part, and they flow toward the Atlantic Ocean; the São Francisco River basin lies in the western part, and it flows inland.

The regional climate is controlled by the high relief of the SER (from 600 to 1400 m). The precipitation depends on the moisture supply from the Atlantic, with the eastern part characterized by a tropical humid climate and annual precipitation greater than 1500 mm (SEA, 1980). The western part is characterized by a tropical semi-humid climate and annual precipitation between 1200 and 1500 mm. The mean annual temperatures for the entire area range from 19 °C to 21 °C (SEA, 1980).

The vegetation is composed of semideciduous forests (Cerrado), the Atlantic forest and high-altitude rocky grasslands (Campos rupestres and Campos de altitude) (Schaefer, 2008; Valente, 2009). The Cerrado, composed of shrub and tree vegetation, dominates in the western and eastern parts. Dominating the highlands, the grassland vegetation of the Campos rupestres and Campos de altitude (Oliveira and Marques, 2002) constitutes ~80% of the study area. The Atlantic forest is present only in the eastern part at low altitudes and can be characterized as rainforest fragments in which few isolated patches of natural forest are preserved.

These three selected areas also show distinct types of human impact. The Serra do Cipó is a national park that is almost entirely preserved (Schaefer, 2008). Some areas of the Serra Talhada, with granitic bedrock, have agricultural and cattle-raising activities, and the alluvium of the Diamantina Plateau rivers was intensively mined for diamonds from 1714 until the mid-1980s (Chaves and Chambel, 2004).

Geologically, the SER is the result of several tectonic events occurring since the late Paleoproterozoic (Almeida Abreu and Pflug, 1994). The SER is a Paleo-Mesoproterozoic rift-sag basin (Alkmim and Martins-Neto, 2001) located at the western margin of the Araçuaí Orogen (Alkmim et al., 2006), facing the eastern border of the São Francisco Craton (Almeida, 1977). The SER was subjected to folding and thrust faults with W-vergence during the Brazilian orogenesis (Alkmim et al., 2006). This event was initiated in the Late Precambrian (800–480 Ma; Peres et al., 2004), and it reactivated the Neoproterozoic

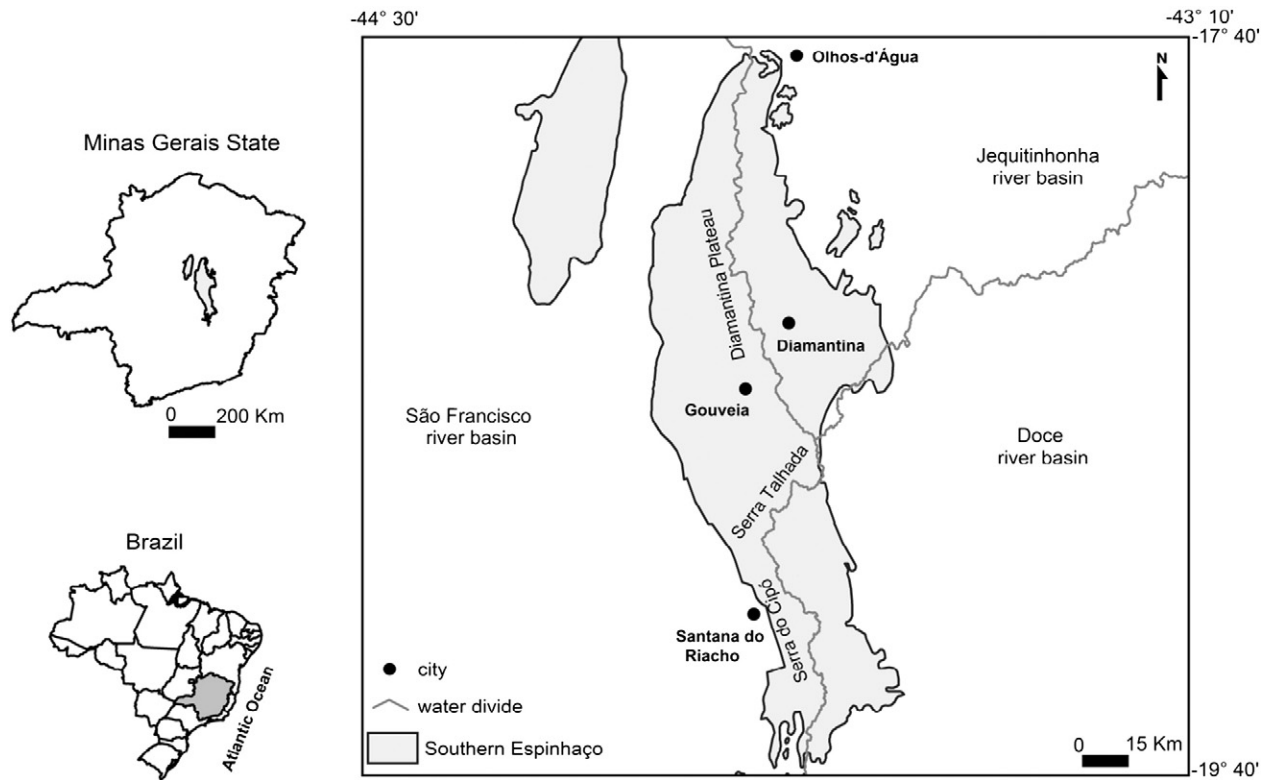


Fig. 2. Map of the Southern Espinhaço, showing the location of the three investigated drainage basins: the Doce, Jequitinhonha and São Francisco.

structures and pushed the basement over the units of the Espinhaço Supergroup from E to W and the Espinhaço Supergroup onto the Bambuí Group (Fig. 3). As a result of this geological evolution, three major rock types (Knauer, 2007) are encountered in the area: the carbonates of the Bambuí Group; quartzite and quartzite associated with quartz-schists from the Espinhaço Supergroup, the most widely exposed rock in the area; and granite-gneiss from the Complex Basal.

The western escarpment of the SER is characterized by a thrust fault front, and the eastern escarpment is structured by a system of thrust faults (Oliveira and Alkimim, 1994). The basement at the southeastern part of the SER shows lower altitudes as a consequence of a Quaternary distensive tectonic, expressed by a graben lake system at the Doce River's middle valley (Suguio and Kholer, 1992; Mello et al., 1999). Three regional designations are used to identify the parts of the SER: the Serra do Cipó in the southern part, with a width of ~30 km; the Serra Talhada (see the geologic section in Fig. 3) in the central part, with a width of ~25 km; and the Diamantina plateau in the northern part, with an average altitude of 1300 m and a width of ~70 to 90 km. The Pico do Itambé summit, with an altitude of 2062 m, is located near the city of Diamantina.

3. Sampling and methods

Before the final selection of an area for river sediment sampling, several investigations were performed. First, 1:50,000 scale topographic maps (Projeto Geominas, 1996) combined with 1:100,000 scale geological maps (Grossi-Sad et al., 1997) were analyzed using ArcGIS 9.2 software, and a 90-m-resolution digital elevation model (DEM) for the study area was extracted from Shuttle Radar Topographic Mission (SRTM) data. Some ArcGIS procedures and the DEM were used to derive the geomorphic parameters for each identified catchment: the maximum elevation (m), average elevation (m), catchment relief elevation (difference between the highest point and the potential sampling point), mean slope gradient (deg), and

catchment area (km²). Then, catchments that are representative of the eastern and western sides of the SER (Fig. 4) and that showed promise as sampling areas were selected based on these geomorphic investigations and field observations. The selection criteria were the following: (i) the eastern and western catchments should have a similar area, (ii) the substratum must be predominantly quartzites, and (iii) the collected samples for each pair of catchments must be equidistant from the divide. Based on these criteria, twelve pairs of catchments were selected on the eastern (the Doce and Jequitinhonha River basins) and western (the São Francisco River basin) sides. In addition, three catchments with a large area were chosen to assess the potential effect of the catchment area on the estimated denudation rate.

In the southern part, the eastern samples from the Doce River basin (D01 to D07) (Serra do Cipó and Serra Talhada) face the western samples from the São Francisco River basin (SF01 to SF08). In the northern part, the eastern samples from the Jequitinhonha River basin (J01 to J05) face the western samples from the São Francisco River basin (SF10, SF11, SF12, SF13 and SF15). In the middle part (Serra Talhada), the eastern sample from the Doce River basin (D08) faces the western sample from the São Francisco River basin (SF9) (Fig. 4).

Most of the selected catchments have surface areas ranging from ~6 to 140 km² (Table 1). The three large catchments (Table 1) correspond to the Cipó (SF6, 239.8 km²), Pardo Grande (SF15, 733.9 km²) and Jequitinhonha (J03, 911.7 km²) rivers. The sample elevations varied from ~580 to 1300 m. The maximum elevation for the catchments was 2021 m (J03), and the minimum elevation was 592 m (D05).

Active sediments transported through catchments predominantly drain the Southern Espinhaço highlands quartzite lithology; however, other lithologies, such as schist, phyllite, granite-gneiss and carbonate, can be associated to some extent. According to geological maps from the Espinhaço Project mapping (1:100,000, Grossi-Sad et al., 1997), the principal lithological types were grouped into five classes (Table 2): (i) predominance of quartzites, (ii) predominance of quartzites associated with schist and phyllite, (iii) granite-gneiss, (iv) intrusive

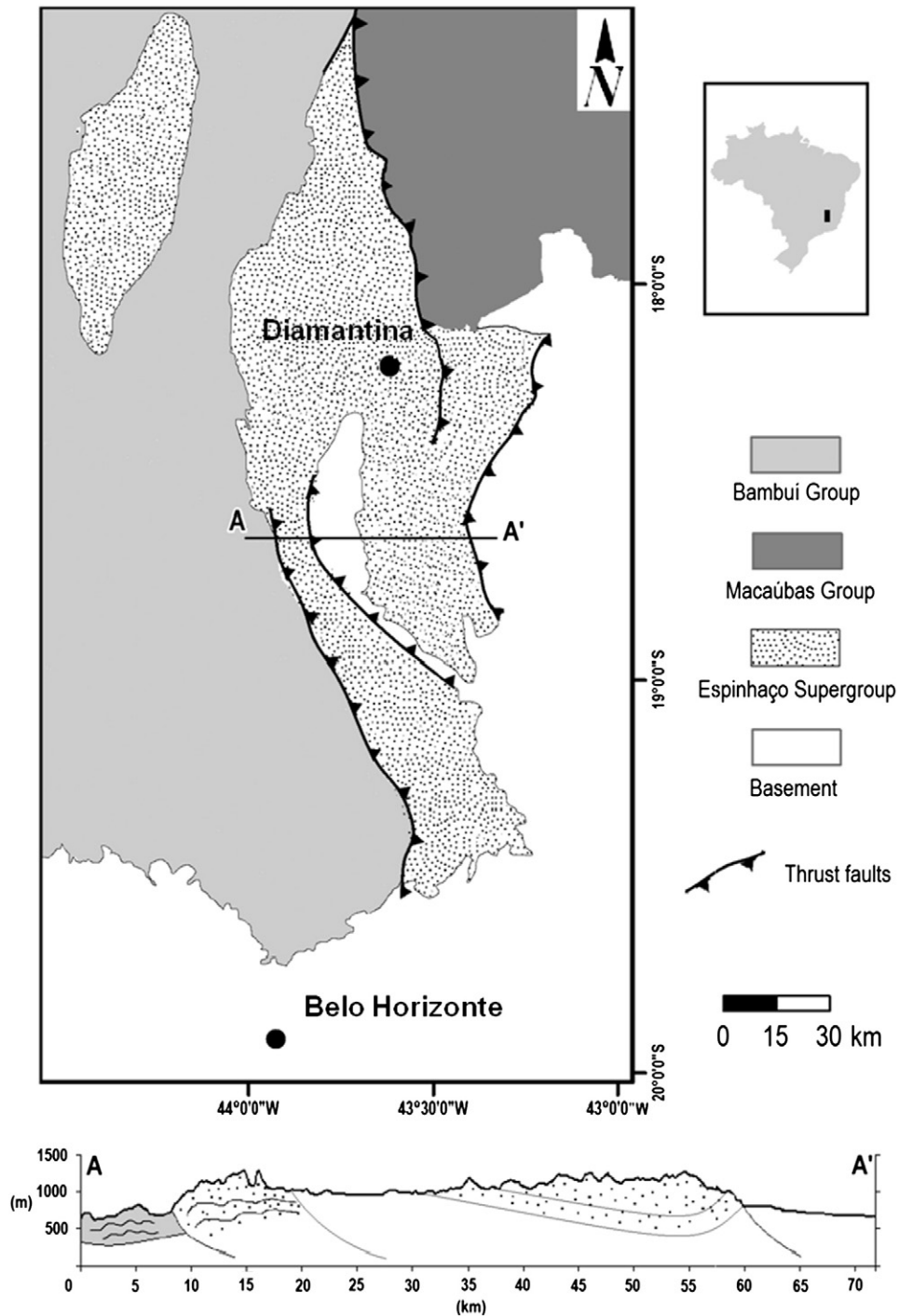


Fig. 3. Geologic map of the Southern Espinhaço (modified from Alkmim et al., 2006). Modified from Alkmim et al. (2006).

igneous rocks, and (v) carbonate rocks. Thus, we calculated the participation ($\text{km}^2\%$) of each lithostratigraphic unit (Table 2) compared with the total area of the catchment. For these results, we used the average density of the rock (g cm^{-3}) for each catchment according to the types of rock (Telford et al., 1990) that occur in their catchment area (Fig. 5).

4. Laboratory analysis

Chemical treatment of the samples and AMS measurements were performed at the LN2C French national laboratory, hosted by CEREGE (Aix-en-Provence). The samples were prepared for cosmogenic nuclide concentration measurements following chemical procedures

Fig. 4. Sampling locations in the Southern Espinhaço. A) Southern Espinhaço Range. B) Detail of sampling points for the northern part (Diamantina Plateau). C) Detail of sampling points for the middle part (Serra Talhada). D) Detail of sampling points for the southern part (Serra do Cipó).

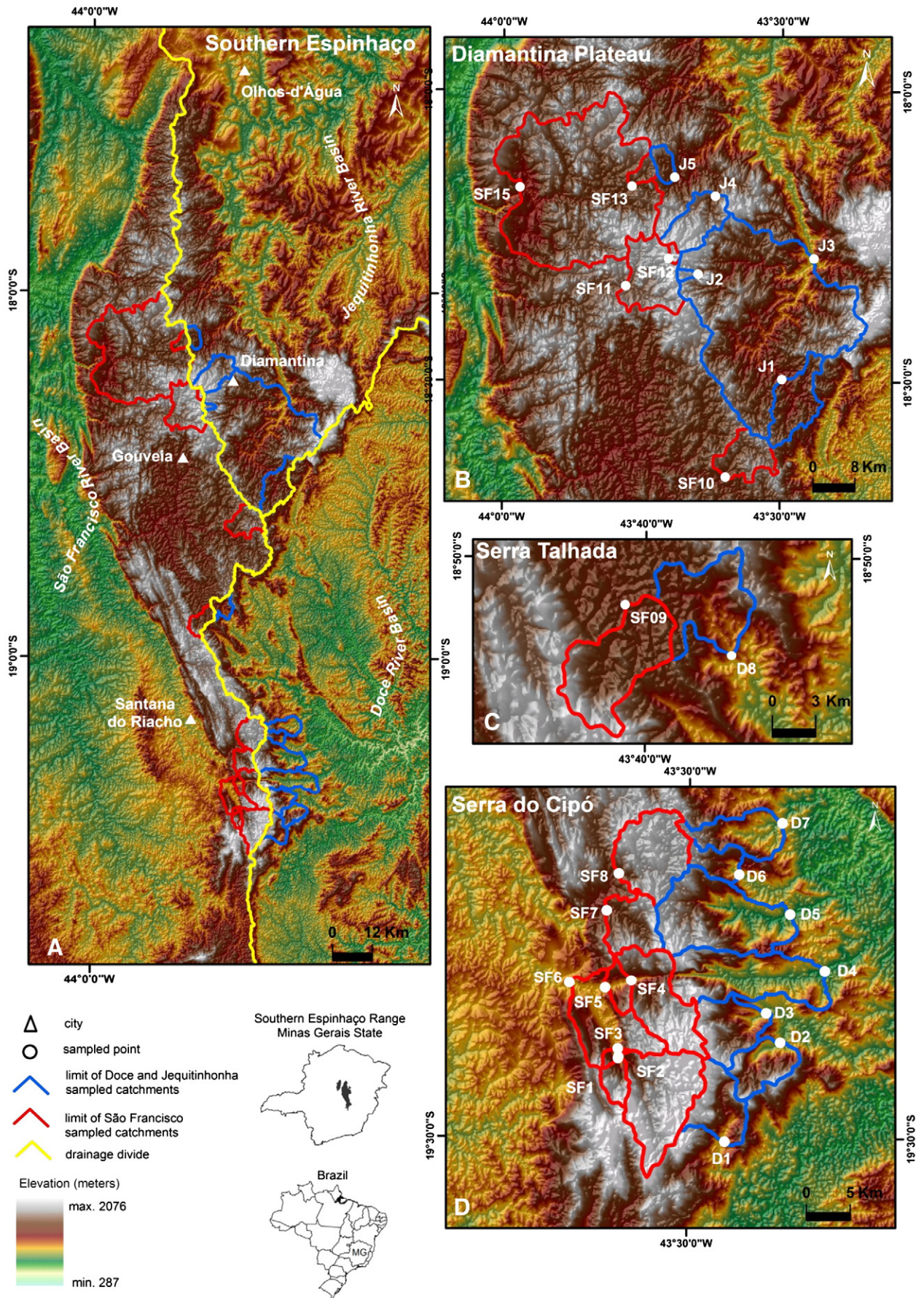


Table 1
Sample locations and geomorphic catchment parameters.

Sampled point	River name	Longitude (W) (WGS84)	Latitude (S) (WGS84)	Sample elevation (m)	Maximum elevation catchments (m)	Minimum elevation catchments (m)	Average elevation catchments (m)	Catchment relief (m)	Mean slope (deg.)	Catchment area (km ²)
D01	Tanque	43.45989	19.504178	768	1610	777	1194	842	13	41.8
D02	Santana	43.40035	19.401618	656	1563	666	1054	907	15	34.8
D03	Preto	43.41569	19.371332	671	1669	682	1160	998	12	45.0
D04	Peixe	43.35257	19.327154	589	1549	599	921	960	13	92.5
D05	Preto de Cima	43.39069	19.268859	587	1541	592	1021	954	11	106.5
D06	Picão	43.44624	19.227906	685	1366	705	1083	681	13	19.3
D07	Mata Cavalos	43.40000	19.174664	628	1382	652	935	754	12	41.3
D08	Lavrinha	43.61026	18.895532	778	1340	793	1035	562	11	32.2
J01	Jequitinhonha	43.49819	18.496547	906	1336	916	1087	430	9	99.6
J02	Canudos	43.65033	18.315596	1264	1539	1277	1359	275	8	6.4
J03	Jequitinhonha	43.44206	18.287900	723	2021	737	1117	1298	9	911.7
J04	Pedras	43.62019	18.181599	1077	1466	1082	1303	389	6	83.1
J05	Areia	43.69335	18.149172	1022	1387	1034	1161	365	6	22.6
SF01	Confins	43.57614	19.418823	804	1583	822	1256	779	12	12.6
SF02	Bandeirinhas	43.57572	19.417567	797	1674	820	1393	877	9	84.9
SF03	Mascates	43.57651	19.408982	796	1674	812	1364	878	9	100.9
SF04	Bocaina	43.56244	19.338524	800	1684	811	1290	884	10	66.0
SF05	Bocaina	43.59071	19.346036	794	1684	801	1250	890	11	78.5
SF06	Cipó	43.62960	19.340948	792	1684	794	1245	892	10	239.8
SF07	Indequiricé	43.58967	19.265994	988	1560	994	1232	572	8	36.4
SF08	Capivara	43.57694	19.227631	1113	1447	1116	1319	334	6	66.6
SF09	Congonhas	43.68078	18.863637	1035	1468	1041	1163	433	8	40.3
SF10	Tijucal	43.59834	18.664776	1030	1345	1056	1200	315	7	73.1
SF11	Pardo Pequeno	43.78010	18.336179	1153	1526	1158	1310	373	6	131.8
SF12	Pasmar	43.70332	18.288937	1300	1460	1310	1391	160	5	6.3
SF13	Begônias	43.76996	18.164859	1091	1364	1099	1179	273	5	18.7
SF15	Pardo Grande	43.97082	18.167377	923	1528	927	1181	605	7	733.9

adapted from Brown et al. (1991) and Merchel and Herpers (1999). Decontaminated quartz minerals were completely dissolved in hydrofluoric acid after the addition of ~100 µl of an in-house $3 \times 10^{-3} \text{ g g}^{-1}$ (⁹Be) carrier solution prepared from a deep-mined phenakite mineral (Merchel et al., 2008). Beryllium was subsequently

separated from the solution by successive anionic and cationic resin extraction (DOWEX 1X8, then 50WX8) and precipitation. The final precipitate was dried and heated at 800 °C to obtain BeO and was finally mixed with niobium for target packing. The samples were analyzed by accelerator mass spectrometry (AMS) at the French

Table 2
The percentage area of the main lithologies in the sampled catchments from the Southern Espinhaço and their respective densities.

Sampled point	River name	Lithologies (%)					Average density according to rock type substratum of each catchment g cm ⁻³
		Quartzites $d = 2.65 \text{ g cm}^{-3}$	Schists and phyllites $d = 2.69 \text{ g cm}^{-3}$	Intrusive rocks $d = 2.99 \text{ g cm}^{-3}$	Granite-gneiss $d = 2.72 \text{ g cm}^{-3}$	Carbonate rocks $d = 2.55 \text{ g cm}^{-3}$	
D01	Tanque	97.3	–	–	2.7	–	2.65
D02	Santana	85.2	–	14.8	–	–	2.70
D03	Preto	100.0	–	–	–	–	2.65
D04	Peixe	98.5	–	1.5	–	–	2.66
D05	Preto de Cima	96.8	–	3.2	–	–	2.66
D06	Picão	98.2	–	1.8	–	–	2.65
D07	Mata Cavalos	84.1	4.2	9.1	1.5	–	2.68
D08	Lavrinha	24.2	–	6.8	69.0	–	2.72
SF01	Confins	97.5	2.5	–	–	–	2.65
SF02	Bandeirinhas	97.2	0.4	2.5	–	–	2.66
SF03	Mascates	96.5	1.5	2.1	–	–	2.65
SF04	Bocaina	79.6	15.3	5.1	–	–	2.67
SF05	Bocaina	75.8	19.9	4.3	–	–	2.67
SF06	Cipó	83.5	12.5	1.3	–	1.8	2.65
SF07	Indequiricé	23.2	73.9	2.9	–	–	2.69
SF08	Capivara	91.0	2.4	6.6	–	–	2.67
SF09	Congonhas	51.8	–	11.9	36.3	–	2.71
J01	Jequitinhonha	68.4	9.8	21.8	–	–	2.72
J02	Canudos	49.6	50.4	–	–	–	2.67
J03	Jequitinhonha	82.3	11.1	5.8	0.8	–	2.67
J04	Pedras	98.6	1.4	–	–	–	2.65
J05	Areia	98.9	–	1.1	–	–	2.65
SF10	Tijucal	86.7	–	13.3	–	–	2.69
SF11	Pardo Pequeno	87.1	11.1	1.4	0.4	–	2.65
SF12	Pasmar	37.28	62.63	–	–	–	2.68
SF13	Begônias	99.3	–	0.6	–	–	2.65
SF15	Pardo Grande	80.6	18.4	1.0	–	–	2.66

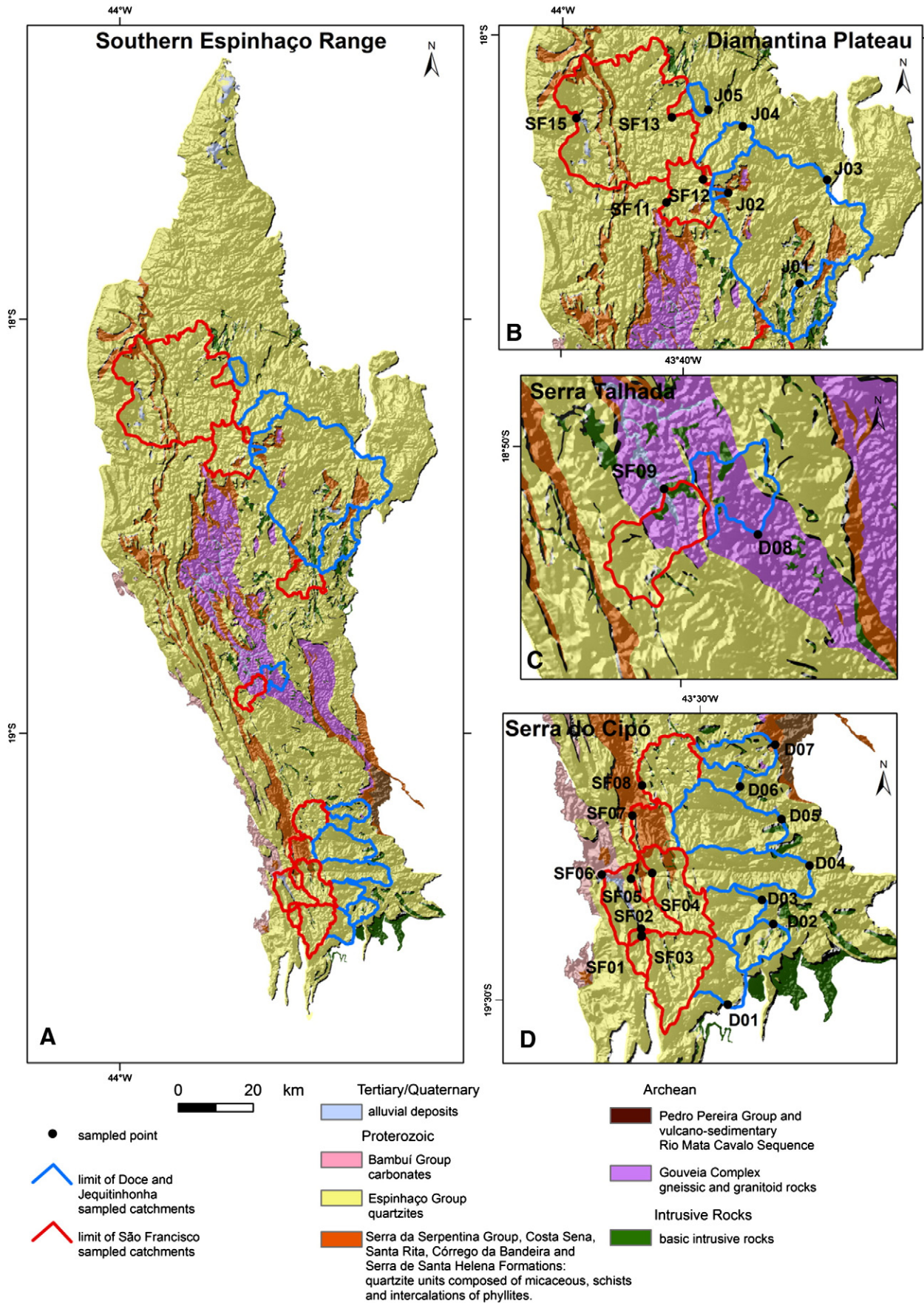


Fig. 5. Geologic map of the Southern Espinhaço. A) Only the principal lithologies are shown. Quartzite rocks are the substratum of most of the catchments investigated (modified from Grossi-Sad et al., 1997). B) Detail of the geology of the northern part (Diamantina Plateau). C) Detail of the geology of the middle part (Serra Talhada). D) Detail of the geology of the southern part (Serra do Cipó).

Table 3
Cosmogenic nuclide results for the Serra do Cipó and Serra Talhada alluvial samples.

Sampled point	Longitude (W) (WGS84) (deg.)	Latitude (S) (WGS84) (deg.)	Average elevation (m)	Scaling factor	^{10}Be concentration (atoms g^{-1})	Uncertain ^{10}Be concentration (atoms g^{-1})	^{10}Be denudation rate (quartz) (m My^{-1})
D01	43.45989	19.504178	1194	1.65	9.02E+05	± 0.27	5.29 \pm 0.16
D02	43.40035	19.401618	1054	1.49	1.20E+06	± 0.04	3.46 \pm 0.11
D03	43.41569	19.371332	1160	1.61	1.03E+06	± 0.03	4.45 \pm 0.13
D04	43.35257	19.327154	921	1.34	7.52E+05	± 0.20	5.27 \pm 0.14
D05	43.39069	19.268859	1021	1.45	1.02E+06	± 0.03	4.04 \pm 0.12
D06	43.44624	19.227906	1083	1.52	1.00E+06	± 0.03	4.31 \pm 0.13
D07	43.40000	19.174664	935	1.35	6.54E+05	± 0.19	6.30 \pm 0.18
D08	43.61026	18.895532	1035	1.46	7.04E+05	± 0.22	6.14 \pm 0.20
SF01	43.57614	19.418823	1256	1.73	9.90E+05	± 0.29	4.99 \pm 0.15
SF02	43.57572	19.417567	1393	1.91	1.94E+06	± 0.06	2.59 \pm 0.08
SF03	43.57651	19.408982	1364	1.87	1.52E+06	± 0.04	3.35 \pm 0.09
SF04	43.56244	19.338524	1290	1.77	1.36E+06	± 0.04	3.60 \pm 0.11
SF05	43.59071	19.346036	1250	1.72	1.23E+06	± 0.04	3.90 \pm 0.12
SF06	43.62960	19.340948	1245	1.71	9.09E+05	± 0.28	5.44 \pm 0.17
SF07	43.58967	19.265994	1232	1.69	2.36E+06	± 0.07	1.80 \pm 0.05
SF08	43.57694	19.227631	1319	1.80	1.99E+06	± 0.05	2.37 \pm 0.05
SF09	43.68078	18.863637	1163	1.60	9.51E+05	± 0.29	4.84 \pm 0.15

AMS national facility ASTER. All ^{10}Be concentrations are normalized to $^{10}\text{Be}/^9\text{Be}$ SRM 4325 NIST reference material with an assigned value of $2.79 \pm 0.03 \times 10^{-11}$.

The analytical uncertainties (reported as 1σ) include those associated with AMS counting statistics, AMS internal error (0.5%) and chemical blank measurement. Long-term measurements of chemically processed blank yield ratios are on the order of $3.0 \pm 1.5 \times 10^{-15}$ for ^{10}Be (Arnold et al., 2010). The Cosmocalc add-in for Microsoft Excel (Vermeesch, 2007) was used to calculate sample thickness scaling (with an attenuation coefficient of 150 g cm^{-2}) and atmospheric pressures. The polynomial function proposed by Stone (2000) was used to determine the surface production rate, assuming a sea level high latitude (SLHL) production rate of $4.49 \text{ at g}^{-1} \text{ yr}^{-1}$ for ^{10}Be (half-life $1.387 \times 10^6 \text{ My}$) (Chmeleff et al., 2010; Korschinek et al., 2010).

Surface cosmogenic nuclide production rates can be affected by potential shielding. If topographic obstructions block the incident cosmic radiation-producing cosmogenic nuclides before they reach a sample location, a decrease in the cosmic-ray flux corresponds to a production rate in this sample lower than that calculated from the spatially scaled SLHL production rate, which only considers unshielded exposure. Thus, for each sample, it is necessary to determine the percentage of cosmic-ray flux effectively producing cosmogenic nuclides relative to the cosmic-ray flux corresponding to an unobstructed view of the sky in all directions. These calculations were numerically performed using the approach of Dunne et al. (1999), and the DEM of the studied area was applied. Because the studied catchments are generally open and

have low mean slopes (Table 2), the shielding factors (equivalent to the fraction of open sky) associated with the discussed samples are close to 1, and the decrease of their production rates induced by the surrounding topography is negligible.

The denudation rates were determined from the measured in-situ-produced cosmogenic ^{10}Be concentrations using the following equation:

$$C_{(x,\varepsilon,t)} = \frac{P_{\text{spall}}}{\varepsilon + \lambda} e^{-\frac{x}{\Lambda_n}} \left[1 - \exp\left\{-t\left(\frac{\varepsilon}{\Lambda_n} + \lambda\right)\right\} \right] + \frac{P_{\mu_{\text{slow}}}}{\varepsilon + \lambda} e^{-\frac{x}{\Lambda_{\mu_s}}} \left[1 - \exp\left\{-t\left(\frac{\varepsilon}{\Lambda_{\mu_s}} + \lambda\right)\right\} \right] + \frac{P_{\mu_{\text{fast}}}}{\varepsilon + \lambda} e^{-\frac{x}{\Lambda_{\mu_f}}} \left[1 - \exp\left\{-t\left(\frac{\varepsilon}{\Lambda_{\mu_f}} + \lambda\right)\right\} \right],$$

where $C_{(x,\varepsilon,t)}$ is the ^{10}Be concentration as a function of depth x (g cm^{-2}); ε is the erosion rate ($\text{g cm}^{-2} \text{ yr}^{-1}$); t is the exposure time (yr); P_{spall} is the production from neutron-induced spallation reaction; $P_{\mu_{\text{slow}}}$ and $P_{\mu_{\text{fast}}}$ are the relative production rates arising from slow and fast muons, assuming relative contributions to the total surface production rate of $1.2 \pm 0.6\%$ and $0.65 \pm 0.25\%$, respectively, for

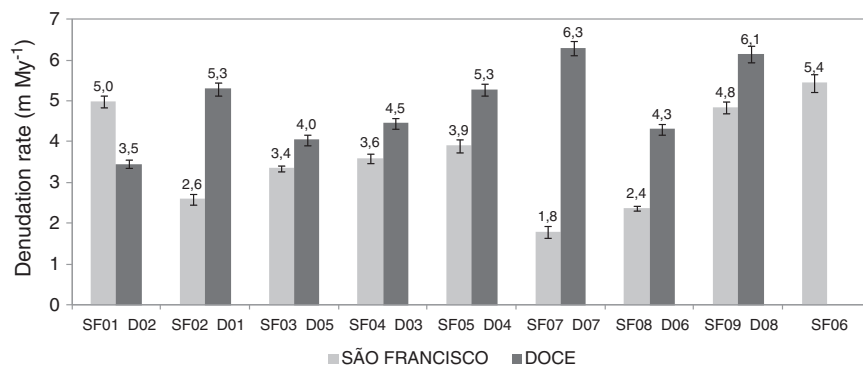


Fig. 6. Denudation rates of Serra do Cipó and Serra Talhada. Each pair of bars (dark and light gray) corresponds to the facing catchments on the western (light gray) and eastern (dark gray) sides of the Southern Espinhaço.

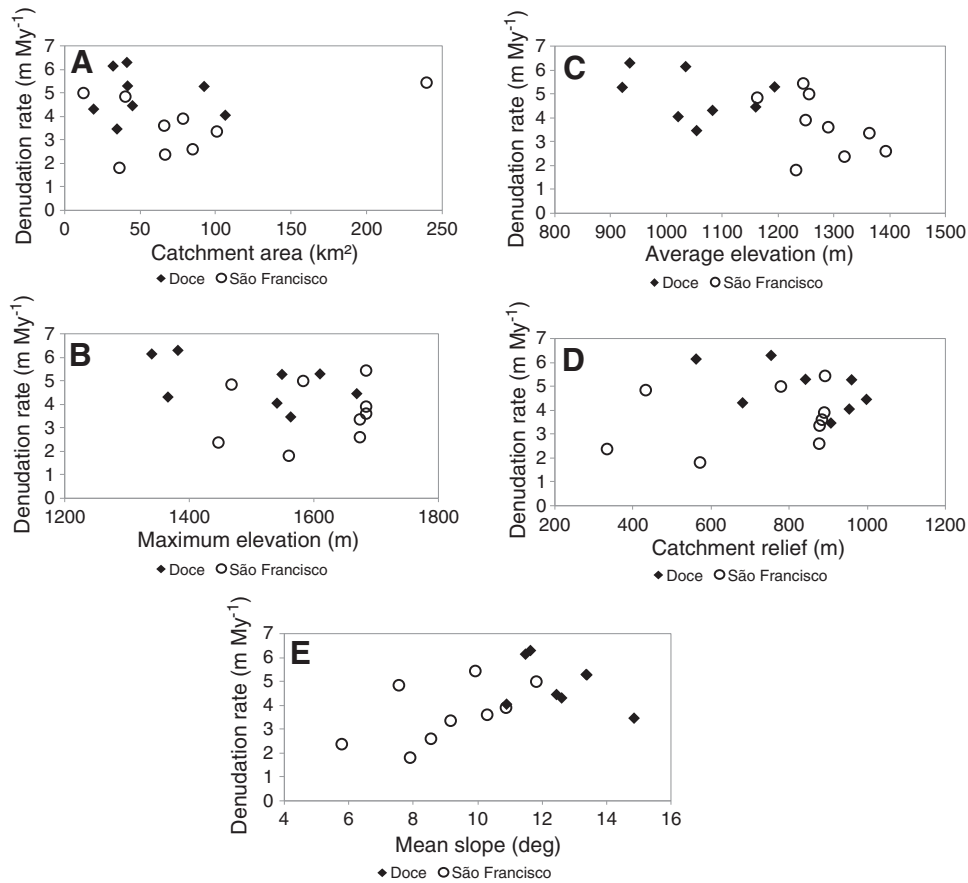


Fig. 7. Relationships between catchment-averaged denudation rates and physical parameters for Serra do Cipó and Serra Talhada. A) catchment area; B) maximum elevation; C) average elevation; D) catchment relief; and E) mean slope.

slow and fast muons that are 0.038 ± 0.019 at $\text{gSiO}_2^{-1} \text{yr}^{-1}$ and 0.027 ± 0.010 at $\text{gSiO}_2^{-1} \text{yr}^{-1}$, respectively (Braucher et al., 2003); and Λ_n , Λ_{ls} , and Λ_{lf} are the effective apparent attenuation lengths (g cm^{-2}) for neutrons and slow and fast muons, respectively. All calculations were performed using attenuation lengths of 160, 1500, and 4320 g cm^{-2} .

5. Results

5.1. Serra do Cipó and Serra Talhada

The results from the Serra do Cipó and Serra Talhada were collected from 17 catchments (Fig. 4; Table 3). The denudation rates of the facing catchments (western and eastern) are presented in Fig. 6. The

denudation rates for the Doce River basin range from 3.5 ± 0.1 to $6.3 \pm 0.1 \text{ m My}^{-1}$, with a mean value of $4.91 \pm 1.01 \text{ m My}^{-1}$. The denudation rates for the São Francisco River basin vary from 1.8 ± 0.05 to $5.4 \pm 0.17 \text{ m My}^{-1}$, with a mean value of $3.65 \pm 1.26 \text{ m My}^{-1}$. The result for the Doce River basin shows denudation rates slightly higher than those of the São Francisco River basin.

If the catchment areas are plotted against the denudation rates (Fig. 7A), the denudation rates are similar for the small and large catchments. The ¹⁰Be concentrations measured in the largest catchment area (239.8 km^2) from the Cipó catchment (SF06) yield an average denudation rate of $5.44 \pm 0.17 \text{ m My}^{-1}$, whereas the denudation rate calculated for the smallest catchment area (SF01) is $4.99 \pm 0.15 \text{ m My}^{-1}$. There seems to be no correlation between drainage area and the denudation rates, despite the geomorphic differences

Table 4
Cosmogenic nuclide results for the Diamantina Plateau alluvial samples.

Sampled point	Longitude (W) (WGS84) (deg.)	Latitude (S) (WGS84) (deg.)	Average elevation (m)	Scaling factor	¹⁰ Be concentration (atoms g ⁻¹)	Uncertain ¹⁰ Be concentration (atoms g ⁻¹)	¹⁰ Be denudation rate (quartz) (m My ⁻¹)
J01	43.49819	18.496547	1087	1.51	8.67E+05	±0.25	5.05 ± 0.15
J02	43.65033	18.315596	1359	1.84	1.60E+06	±0.05	3.10 ± 0.09
J03	43.44206	18.287900	1117	1.54	9.17E+05	±0.29	4.84 ± 0.15
J04	43.62019	18.181599	1303	1.76	1.39E+06	±0.04	3.49 ± 0.11
J05	43.69335	18.149172	1161	1.59	8.31E+05	±0.24	5.56 ± 0.16
SF10	43.59834	18.664776	1200	1.64	1.12E+06	±0.03	4.13 ± 0.12
SF11	43.78010	18.336179	1310	1.77	1.81E+06	±0.06	2.60 ± 0.08
SF12	43.70332	18.288937	1391	1.88	1.42E+06	±0.04	3.66 ± 0.11
SF13	43.76996	18.164859	1179	1.61	9.26E+05	±0.29	5.01 ± 0.16
SF15	43.97082	18.167377	1181	1.61	1.04E+06	±0.03	4.43 ± 0.14

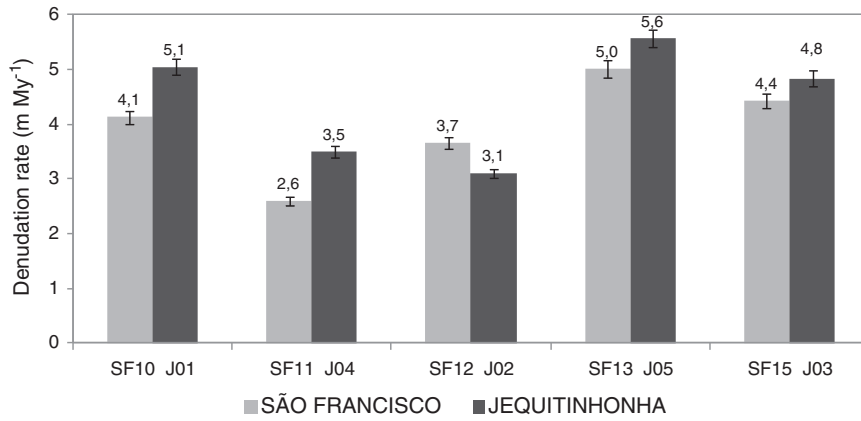


Fig. 8. Denudation rates of the Diamantina Plateau. Each pair of bars (dark and light gray) corresponds to facing catchments on the western (light gray) and eastern (dark gray) sides of the Southern Espinhaço.

between these catchments in terms of their maximum elevation, catchment relief or slope gradients (Table 1). The same conclusion applies if the denudation rates are plotted against these parameters (Fig. 7B,D,E). The average elevation parameter for the catchments in the Doce basin (~900 to 1200 m) was lower than that of the São Francisco basin (~1150 to 1400 m), as shown in Fig. 7C. However, even the catchments of the Doce River basin showing a lower average

elevation have denudation rates that are slightly higher than those of the São Francisco River basin.

The denudation rates for catchments containing various lithologies (Table 2), such as schists and phyllites (SF04, SF05, SF06, and SF07), carbonates (SF06) or igneous rocks (D08) hosted by quartzites, are similar to those of catchments dominated by quartzites. This result suggests that the less frequent occurrence of other lithologies

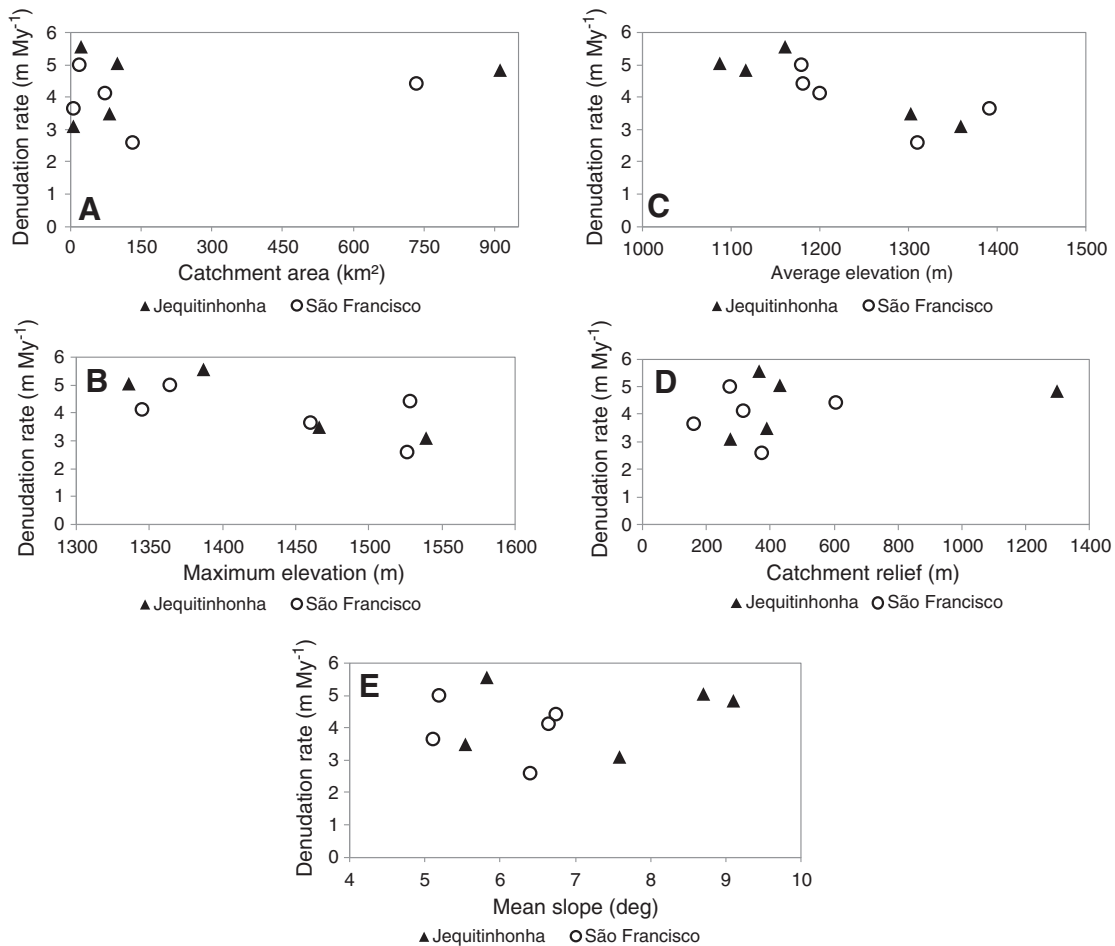


Fig. 9. Relationships between catchment-averaged denudation rates and geomorphic parameters for the Diamantina Plateau. A) catchment area; B) maximum elevation; C) average elevation; D) catchment relief; and E) mean slope.

(less than 15% of the catchment area) does not significantly alter the denudation rates. The results found in the Serra Talhada for samples SF09 ($4.39 \pm 0.135 \text{ m My}^{-1}$) and D08 ($5.08 \pm 0.162 \text{ m My}^{-1}$) correspond to catchments underlain by two lithologies: quartzites of the Espinhaço Supergroup (SF09: 54% and D08: 33%) and granite-gneiss of the Gouveia Complex (D08: 69% and SF09: 36%). Despite the high percentages of granite-gneiss, the influence of these lithologies was not detected, and the results are similar in comparison with all the data.

5.2. Diamantina Plateau

The results for the sediment samples from the Diamantina Plateau drainage systems were collected from 10 catchments (Fig. 4; Table 4). The denudation rates of the facing catchments on the western and eastern sides of the SER are presented in Fig. 8. The rates for the Jequitinhonha River basin range from 3.1 ± 0.09 to $5.6 \pm 0.16 \text{ m My}^{-1}$ (Table 4), with a mean of $4.40 \pm 1.06 \text{ m My}^{-1}$. The rates of the São Francisco River range from 2.6 ± 0.08 to $5.0 \pm 0.16 \text{ m My}^{-1}$, with a mean of $3.96 \pm 0.91 \text{ m My}^{-1}$. The denudation rates show almost no correlation with the geomorphic parameters (Fig. 9), although four catchments with higher average elevations (1300 to 1400 m) have slightly lower rates. However, these results agree closely with those for the other catchments from the Diamantina Plateau.

6. Discussion

The denudation rates determined in the northern part of the study area are similar to those determined in the southern part. The mean rates are low, ranging from 3.65 to 6.14 m My^{-1} (Fig. 10). Although the Diamantina Plateau catchments have slightly different geomorphic parameters from those of the Serra do Cipó (e.g., the catchment relief and mean slope gradient), the denudation rates are similar for both parts, even in the human-influenced areas of the Diamantina plateau, which were intensively disturbed by alluvium diamond panning in the past.

The mean denudation rate of the 24 small catchments studied ($4.13 \pm 1.19 \text{ m My}^{-1}$) is similar to the results for the largest catchments: (i) in the Diamantina Plateau, the SF15 (733.9 km^2) and the J03 (911.7 km^2) showed denudation rates of $4.43 \pm 0.14 \text{ m My}^{-1}$ and $4.84 \pm 0.15 \text{ m My}^{-1}$, respectively; and (ii) in the Serra do Cipó, the SF06 (239.8 km^2) showed a denudation rate of $5.44 \pm 0.17 \text{ m My}^{-1}$. The examination of these low values reveals the importance of the control exerted by the lithology in a catchment substratum dominated by quartzites.

The slightly higher denudation rates for the Doce River basin can be explained as a consequence of Quaternary base-level changes at the middle Doce River due to distensive tectonic-generating graben structures with dozens of associated lakes (Mello et al., 1999; Riccomini and Assumpção, 1999). The most widely exposed rock in this area is the granite-gneiss of the Complex Basal (Fig. 3), which is less resistant to erosion processes than the quartzites of the Supergroup Espinhaço. The association of both factors, lithological (gneiss) contact and recent tectonic changes, explains the slightly higher denudation rates found for the Doce River catchments. The DEM (Fig. 4) shows the contrast between the dissected granite-gneiss areas (green) and the high-altitude resistant quartzitic areas (orange).

The results for the Serra Talhada catchments (SF09 and D08) attest to the resistance of the quartzites despite the occurrence of the granite-gneiss substratum. Even with the presence of less resistant rocks, the denudation rates are closer to the other results for the SER. The long-term denudation rates found in the Minas Gerais (Brazil) granite-gneiss substratum are the following: $14.9 \pm 2.28 \text{ m My}^{-1}$ (Salgado et al., 2008) in Quadrilátero Ferrífero, $8.77 \pm 2.78 \text{ m My}^{-1}$ in Cristiano Ottoni, and $15.68 \pm 4.53 \text{ m My}^{-1}$ in São Geraldo (Cherem et al., 2012). Studies in the Appalachian Mountains measuring the granite substratum from the Blue Ridge Province showed denudation rates of 7.9 to 21.8 m My^{-1} (Duxbury, 2009), and the gneiss substratum from the Great Smoky Mountains showed values of $\sim 27 \text{ m My}^{-1}$ (Matmon et al., 2003). The low values of the long-term denudation rates confirm that the Serra Talhada granite-gneiss occurrence, protected by resistant quartzite, hardly affects the denudation rates.

Most of the denudation rates obtained are lower than 5 m My^{-1} and are consistent with those measured in other catchments that drain quartzites: (i) in the Quadrilátero Ferrífero (Brazil), with values ranging from 1.07 ± 0.13 to $3.18 \pm 0.31 \text{ m My}^{-1}$ (Salgado et al., 2006, 2008); (ii) in the Shenandoah National Park (Appalachian Mountains), with values ranging from 4.7 to 16.8 m My^{-1} (Duxbury, 2009); and (iii) in the Central Highlands of Sri Lanka, with values ranging from 5 to 8 m My^{-1} for the Galaha River (Von Blanckenburg et al., 2004).

The denudation rates obtained in this study suggest no direct correlation if plotted against geomorphic parameters such as catchment area, maximum elevation, catchment relief, average relief and mean slope. These results are supported by recent studies using cosmogenic nuclides. In the Rio Puerco basin (New Mexico), Bierman et al. (2005) found a weak relationship between denudation rates and relief in sandstone, shale, granitic and volcanic substrata. In the Great Smoky Mountains (North Carolina and Tennessee), Matmon et al. (2003) found no relationship between denudation rates and drainage area or maximum and average elevation in sandstone and slate substrata.

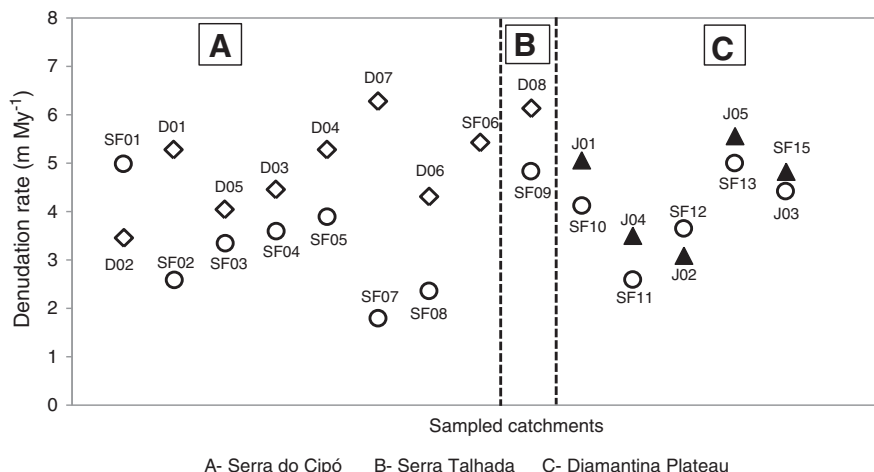


Fig. 10. ¹⁰Be denudation rates for the Southern Espinhaço.

7. Summary

In situ-produced cosmogenic ^{10}Be concentrations measured in river sediments enabled the determination of long-term denudation rates in the SER. The obtained results show low values ($<5\text{ m My}^{-1}$), irrespective of the geomorphic differences between the studied areas. The similarity of the results emphasizes the importance of resistant quartzitic lithologies as the primary controlling variable for denudation rates. The low denudation rates also show how slowly the regional landscape, which is characterized by substantial resistant and residual relief, has evolved in the past 1.38 My.

Acknowledgments

The authors are grateful to CAPES/COFECUB, CNPq and FAPEMIG for funding this research; to Laëtítia Leanni for her help during the chemical preparations; and to Maurice Arnold, Georges Aumaître and Karim Keddadouche for their invaluable help with the ^{10}Be AMS measurements.

References

- Alkmim, F.F., Martins-Neto, M.A., 2001. A Bacia Intracratônica do São Francisco arcabouço estrutural e cenários evolutivos. In: Pinto, C.P., Martins-Neto, M.A. (Eds.), *Bacia do São Francisco geologia e recursos naturais*. Belo Horizonte, SBG-MG, pp. 9–30.
- Alkmim, F.F., Marshak, S., Pedrosa-Soares, A.C., Peres, G.G., Cruz, S.C.P., Whittington, A., 2006. Kinematic evolution of the Araçuaí–West Congo orogen in Brazil and Africa: Nutcracker tectonics during the Neoproterozoic assembly of West Gondwana. *Precambrian Research* 149, 43–64.
- Almeida, F.F.M., 1977. O Cráton do São Francisco. *Revista Brasileira Geociências* 7, 349–364.
- Almeida Abreu, P.A., 1995. O Supergrupo Espinhaço da Serra do Espinhaço Meridional (Minas Gerais): o rifte, a bacia e o orógeno. *Geonomos* 3 (1), 1–18.
- Almeida Abreu, P.A., Pflug, R., 1994. The geodynamic evolution of the Southern Serra do Espinhaço, Minas Gerais, Brazil. *Zbl. Geol. Paläont., Teil I*, 1/2, pp. 21–44.
- Arnold, M., Merchel, S., Bourlés, D.L., Braucher, R., Benedetti, L., Finkel, R.C., Aumaître, G., Gottang, A., Klein, M., 2010. The French accelerator mass spectrometry facility ASTER: improved performance and developments. *Nuclear Instruments and Methods in Physics Research B* 268, 1954–1959.
- Bierman, P.R., Steig, E., 1996. Estimating rates of denudation and sediment transport using cosmogenic isotope abundances in sediment. *Earth Surface Processes and Landforms* 21, 125–139.
- Bierman, P.R., Reuter, J.M., Pavich, M., Gellis, A.C., Caffee, M.W., Larsen, J., 2005. Using cosmogenic nuclides to contrast rates of erosion and sediment yield in a semi-arid, arroyo-dominated landscape, Rio Puerco Basin, New Mexico. *Earth Surface Processes and Landforms* 30, 935–953.
- Braucher, R., Brown, E.T., Bourlés, D.L., Colin, F., 2003. In situ-produced ^{10}Be measurements at great depths – implications for production rates by fast muons. *Earth and Planetary Science Letters* 211, 251–258.
- Brown, E.T., Edmond, J.M., Raisbeck, G.M., Yiu, F., Kurz, M.D., Brook, E.J., 1991. Examination of surface exposure ages of Antarctic moraines using in situ produced ^{10}Be and ^{26}Al . *Geochimica et Cosmochimica Acta* 55, 2269–2283.
- Brown, E.T., Stallard, R.F., Larsen, M.C., Raisbeck, G.M., Yiu, F., 1995. Denudation rates determined from the accumulation of in-situ produced ^{10}Be in the Luquillo Experimental Forest, Puerto Rico. *Earth and Planetary Science Letters* 129, 193–202.
- Caine, N., 2004. Mechanical and chemical denudation in mountain systems. In: Owens, P.N., Slaymaker, O. (Eds.), *Mountain Geomorphology*. Oxford University Press, Oxford, pp. 132–152.
- Chaves, M.L.S.C., Chambel, L., 2004. Diamantes do médio rio Jequitinhonha, Minas Gerais – qualificação gemológica e análise granulométrica. *Revista Escola de Minas* 57, 267–275.
- Cherem, L.F.S., Varajão, C.A.C., Braucher, R., Bourlés, D., Salgado, A.A.R., Varajão, A.F.D.C., 2012. Long-term evolution of denudational escarpments in southeastern Brazil. *Geomorphology* 173–174, 118–127.
- Chmeleff, J., Blanckenburg, F.V., Kossert, K., Jakob, D., 2010. Determination of the ^{10}Be half-life by multicollector ICP-MS and liquid scintillation counting. *Nuclear Instruments and Methods in Physics Research Section B: Beam Interactions with Materials and Atoms* 268, 192–199.
- Dunne, J., Elmore, D., Muzikar, P., 1999. Scaling factors for the rates of production of cosmogenic nuclides for geometric shielding and attenuation at depth on sloped surfaces. *Geomorphology* 27, 3–11.
- Dussin, I.A., Dussin, T., 1995. Supergrupo Espinhaço, modelo de evolução geodinâmica. *Geonomos* 3 (1), 64–71.
- Duxbury, J., 2009. Erosion rates in and around Shenandoah National Park, VA, determined using analysis of cosmogenic ^{10}Be . PhD thesis, University of Vermont, 123 p.
- Granger, D.E., Riebe, C.S., 2007. Cosmogenic nuclides in weathering and erosion. In: Drever, J.I. (Ed.), *Treatise on Geochemistry, Surface and Ground Water, Weathering, and Soils*, 5. Elsevier, Amsterdam, pp. 1–43.
- Granger, D.E., Kirchner, J.W., Finkel, R.C., 1996. Spatially averaged long-term erosion rates measured from in situ produced cosmogenic nuclides in alluvial sediment. *Journal of Geology* 104, 249–257.
- Granger, D.E., Riebe, C.S., Kirchner, J.W., Finkel, R.C., 2001. Modulation of erosion on steep granitic slopes by boulder armoring, as revealed by cosmogenic ^{26}Al and ^{10}Be . *Earth and Planetary Science Letters* 186, 269–281.
- Grossi-Sad, J.H., Lobato, L.M., Pedrosa-Soares, A.C., Soares-Filho, B.S. (coordenadores e editores), 1997. *Projeto Espinhaço em CD-ROM (textos, mapas e anexos)*. Belo Horizonte: COMIG – Companhia Mineradora de Minas Gerais.
- King, L.A., 1956. *Geomorfologia do Brasil Oriental*. Revista Brasileira de Geociências 18, 147–256.
- Knauer, G., 2007. O Supergrupo Espinhaço em Minas Gerais: considerações sobre sua estratigrafia e seu arranjo estrutural. *Geonomos* 15 (1), 81–90.
- Korschinek, G., Bergmaier, A., Faestermann, T., Gerstmann, U.C., Knie, K., Rugel, G., Wallner, A., Dillmann, I., Dollinger, G., Lierse von Gosstowski, C., Kossert, K., Maiti, M., Poutivsev, M., Remmert, A., 2010. A new value for the ^{10}Be half-life by heavy-ion elastic recoil detection and liquid scintillation counting. *Nuclear Instruments and Methods in Physics Research Section B: Beam Interactions with Materials and Atoms* 268, 187–191.
- Matmon, A., Bierman, P.R., Larsen, J., Southworth, S., Pavich, M., Finkel, R., Caffee, M., 2003. Erosion of ancient mountain range, the Great Smoky Mountains, North Carolina and Tennessee. *American Journal of Science* 303, 817–855.
- Mello, C.L., Metelo, C.M.S., Suguio, K., Kholer, H.C., 1999. Quaternary sedimentation, neotectonics and evolution of Doce River middle valley lake system (Southeastern Brazil). *Revista do Instituto Geológico* 20 (1/2), 29–36.
- Merchel, S., Hergers, U., 1999. An update on radiochemical separation techniques for the determination of long-lived radionuclides via accelerator mass spectrometry. *Radiochimica Acta* 84, 215–219.
- Merchel, S., Arnold, M., Aumaître, G., Benedetti, L., Bourlés, D.L., Braucher, R., Alfimov, V., Freeman, S.P.H.T., Steier, P., Wallner, A., 2008. Towards more precise ^{10}Be and ^{36}Cl data from measurements at the 10–14 level: influence of sample preparation. *Nuclear Instruments and Methods in Physics Research B* 266, 4921–4926.
- Oliveira, F.V.C., Alkmim, F.F., 1994. Estilo estrutural e curvatura da porção sul do fronto do Espinhaço. 38º Congresso Brasileiro de Geologia, Boletim de Resumos Expandidos, Camboriú, 2, pp. 259–260.
- Oliveira, P.S., Marques, R.J., 2002. *The Cerrado of Brazil: Ecology and Natural History of a Neotropical Savanna*. Columbia University Press, New York.
- Peres, G.G., Alkmim, F.F., Jordt-Evangelista, H., 2004. The southern Araçuaí belt and the Dom Silvério group: geologic architecture and tectonic significance. *Anais da Academia Brasileira de Ciências* 76, 771–790.
- Projeto Geominas, 1996. *Geoprocessamento em Minas Gerais*. Digitalized topographic maps of Minas Gerais.
- Reuter, J., Bierman, P.R., Pavich, M., Gellis, A., Larsen, J., Finkel, R., 2003. Long-term sediment generation rates derived from ^{10}Be in river sediment of Susquehanna River Basin, in “channeling through time: landscape evolution, land use change, and stream restoration in the lower Susquehanna Basin”. In: Merritts, D., Walter, R., de Wet, A. (Eds.), *Southeastern Friends of the Pleistocene Fall 2003 Guidebook*, pp. 48–55.
- Riccomini, C., Assumpção, M., 1999. Quaternary tectonics in Brazil. *Episodes* 22, 221–225.
- Riebe, C.S., Kirchner, J.W., Granger, D.E., Finkel, R.C., 2000. Erosional equilibrium and disequilibrium in the Sierra Nevada, inferred from cosmogenic ^{26}Al and ^{10}Be in alluvial sediment. *Geology* 28, 803–806.
- Saadi, A., 1995. A geomorfologia da serra do Espinhaço em Minas Gerais e de suas margens. *Geonomos* 3 (1), 41–63.
- Salgado, A.A.R., Braucher, R., Colin, F., Nalini JR., H.A., Varajão, A.F.D.C., Varajão, C.A.C., 2006. Denudation rates of the Quadrilátero Ferrífero (MinasGerais, Brazil): preliminary results from measurements of solute fluxes in rivers and in situ-produced cosmogenic ^{10}Be . *Journal of Geochemical Exploration* 88, 313–317.
- Salgado, A.A.R., Braucher, R., Colin, F., Varajão, A.F.D., Nalini Júnior, H.A., 2008. Relief evolution of the Quadrilátero Ferrífero (Minas Gerais, Brazil) by means of (^{10}Be) cosmogenic nuclei. *Zeitschrift für Geomorphologie* 52, 317–323.
- Schaefer, C.E., 2008. Diagnóstico do meio físico da APA Morro da Pedreira e da Serra do Cipó: subsídios ao plano de manejo. Relatório do Levantamento Pedológico, Geológico e Geomorfológico. Universidade Federal de Viçosa, Viçosa (80 pp.).
- SEA (Secretaria de Estadual da Agricultura), 1980. *Atlas de Zoneamento Agroclimático do Estado de Minas Gerais*. Escala: 1:300.000. Digitized by PRODEMGE, 1996.
- Shaller, M., Von Blanckenburg, F., Houvius, N., Kubik, P.W., 2001. Large-scale erosion rates from in situ-produced cosmogenic nuclides in European river sediments. *Earth and Planetary Science Letters* 188, 441–458.
- Stone, J., 2000. Air pressure and cosmogenic isotope production. *Journal of Geophysical Research* 105, 23,753–23,759.
- Suguio, K., Kholer, H.C., 1992. Quaternary barred lake systems of Doce river (Brazil). *Anais da Academia Brasileira de Ciências* 64, 183–191.
- Summerfield, M.A., 1998. *Global Geomorphology: An Introduction of Study of Landforms*. Longman Scientific and Technical, Essex (537 pp.).
- Telford, W.M., Geldart, L.P., Sheriff, R.E., 1990. *Applied Geophysics*, 2nd ed. Cambridge University Press, Cambridge.
- Uhlein, A., Trompette, R., Alvarenga, C.J.S., 1999. Neoproterozoic glacial and gravitational sedimentation on a continental rifted margin: the Jequitaiá-Macaúbas sequence (Minas Gerais, Brazil). *Journal of South American Earth Science* 12, 435–451.
- Valadão, C.R., 1998. *Evolução de longo termo do relevo do cráton do São Francisco (denudação, paleosuperfícies e movimentos crustais)*. PhD Thesis, Universidade Federal da Bahia, 343 p.
- Valente, E.L., 2009. *Relações solo-vegetação no Parque Nacional da Serra do Cipó, Espinhaço Meridional – Minas Gerais*. Universidade Federal de Viçosa, PhD Thesis, 157p.

- Vermeesch, P., 2007. CosmoCalc: an Excel add-in for cosmogenic nuclide calculations. *Geochemistry, Geophysics, Geosystems* 8, 1–14.
- Von Blanckenburg, F., 2006. The control mechanisms of erosion and weathering at basin scale from cosmogenic nuclides in river sediment. *Earth and Planetary Science Letters* 242, 224–239.
- Von Blanckenburg, F., Hewawasam, T., Kubik, P.W., 2004. Cosmogenic nuclide evidence for low weathering and denudation in the wet, tropical highlands of Sri Lanka. *Journal of Geophysical Research* 109, 1–22.
- Von Eschwege, W.L., 1832a. *Beitrag zur Gerbigskunde Brasiliens*. G. Reimer, Berlin.
- Von Eschwege, W.L., 1832b. *Quadro Geognóstico do Brasil e a provável rocha matriz dos diamantes*. Trad. para o Português e notas por Renger F.E. 2005: *Geonomos*, 13(1,2), pp. 97–109.
- Wittmann, H., von Blanckenburg, W., 2009. Cosmogenic nuclide budgeting of floodplain sediment transfer. *Geomorphology* 109, 246–256.